The Canadian Mineralogist
Vol. 44, pp. 69-86 (2006)

COLUMBITE–TANTALITE-BEARING GRANITIC PEGMATITES FROM THE SERIDÓ BELT, NORTHEASTERN BRAZIL: GENETIC CONSTRAINTS FROM U–Pb DATING AND Pb ISOTOPES

REGINA BAUMGARTNER[§]

Department of Mineralogy, University of Geneva, 13, Rue des Maraîchers, CH–1205 Geneva, Switzerland

ROLF L. ROMER

GeoForschungsZentrum, Telegrafenberg, D–14473 Potsdam, Germany

ROBERT MORITZ

Department of Mineralogy, University of Geneva, 13, Rue des Maraîchers, CH–1205 Geneva, Switzerland

RICARDO SALLET

Universidade Federal do Rio Grande do Norte, 59072–920, Natal, Brazil

MASSIMO CHIARADIA

Department of Mineralogy, University of Geneva, 13, Rue des Maraîchers, CH–1205 Geneva, Switzerland

ABSTRACT

The Seridó Belt, located in the Borborema Province, northeastern Brazil, is well known for its pegmatites and granites. The pegmatites intrude the Seridó Group and show no signs of deformation. They were emplaced along a major NE-trending shear zone during a post-Brasiliano extensional event (550–500 Ma). Homogeneous bodies of pegmatite are barren, whereas the heterogeneous ones have been mined for columbite–tantalite, beryl, gem tourmaline (elbaite), and kaolin. Electron-microprobe analyses reveal that columbite-group minerals have a composition between ferrocolumbite and manganocolumbite. Our U–Pb age determinations on these minerals show that the pegmatites were emplaced between 509.5 ± 2.9 Ma and 514.9 ± 1.1 Ma. As the pegmatites are not deformed, these ages are interpreted as a minimum age for the Brasiliano orogeny in the Seridó Belt. Our U–Pb data on monazite from a spatially related coarse-grained peraluminous granite give an age of 528 ± 12 Ma. The pegmatites are clearly younger than that granite. Lead isotopes from K-feldspar show that the coarse-grained granite and the pegmatites are derived from several separate batches of magma that received variable amounts of Pb from the distinct host-rocks. The heterogeneity in the Pb isotopic compositions is due to *in situ* Pb growth and the geochemically variable host-rocks.

Keywords: granitic pegmatite, columbite–tantalite, U–Pb, Pb isotopes, Brasiliano orogeny, Seridó Belt, Borborema Province, Brazil.

SOMMAIRE

La ceinture Seridó, située dans la province Borborema, au nord-est du Brésil, est bien connue pour ses pegmatites et granites. Les pegmatites sont encaissées dans les roches appartenant au Groupe de Seridó et ne montrent pas de déformation. Elles ont été mises en place le long d'une zone majeure de cisaillement NE durant un épisode extensionnel postérieur à l'orogenèse brésilienne (550–500 Ma). Les pegmatites homogènes sont stériles, tandis que celles possédant une texture hétérogène ont été exploitées pour la columbite–tantalite, le béryl, la tourmaline gemme (elbaïte) et le kaolin. Des analyses obtenues avec une microsonde électronique montrent que les compositions des minéraux du groupe de la columbite varient entre la ferrocolumbite et la manganocolumbite. Des âges U–Pb sur columbite montrent que les pegmatites étudiées ont été mises en place entre 509.5 ± 2.9 Ma et 514.9 ± 1.1 Ma. Etant donné que les pegmatites ne sont pas déformées, on peut interpréter leur âge comme âge minimum de l'orogenèse brésilienne dans la ceinture Seridó. Les données U–Pb sur monazite d'un granite peralumineux à grains grossiers révèlent un âge de 528 ± 12 Ma. De ces datations, il en ressort que les pegmatites sont clairement plus jeunes

§ *E-mail address*: regina.baumgartner@terre.unige.ch

que le granite hyperalumineux. Les isotopes de plomb sur feldspath potassique montrent que le granite hyperalumineux et les pegmatites sont dérivées de plusieurs venues de magma qui ont acquis du Pb en quantités variables des différentes roches encaissantes. L'hétérogénéité des compositions isotopiques du plomb serait dû à une croissance crustale *in situ* des isotopes de Pb et à la composition géochimique variable des roches encaissantes.

Mots-clés: pegmatites granitiques, columbite–tantalite, U–Pb, isotopes de Pb, orogenèse brésilienne, ceinture Seridó, Province de Borborema, Brésil.

Introduction

The Borborema tectonic Province of northeastern Brazil hosts one of the major granitic pegmatite provinces in South America (Putzer 1976). Several Be–Ta–Nb–Li pegmatite fields are located in the Seridó fold belt in the eastern Borborema Province, about 150 km southwest of the town of Natal, Rio Grande do Norte, Brazil (Beurlen 1995, Da Silva *et al*. 1995). The pegmatites show a variety of homogeneous to heterogeneous internal textures. Only heterogeneous pegmatites with a clear zonation are of economic importance. They are mined by *garimperos* for columbite–tantalite, cassiterite, beryl, high-quality kaolin, lepidolite, K-feldspar, and gem-quality tourmaline (Johnston 1945, Beurlen 1995, Da Silva *et al*. 1995).

The little research that has been done on these pegmatites was mainly focused on the geochemical characteristics of the pegmatites (Da Silva 1993, Da Silva *et al*. 1995) and on the identification of uncommon minerals (Rolff 1946). Imprecise K–Ar muscovite, Rb–Sr muscovite, and U–Pb uraninite ages, which may have been modified by fluid–rock interaction or thermal overprint (Agrawal 1986), exist for a few of these pegmatites. These data indicate an age of 450 to 550 Ma for the pegmatites. In this study, we have performed U–Pb dating on columbite–tantalite from heterogeneous pegmatites as well as on monazite from an associated peraluminous coarse-grained granite. Trace-element contents and the chemical composition of K-feldspar, which are helpful in the assessment of the potential for Nb and Ta mineralization in individual pegmatites (Beus 1966, Gordiyenko 1970, Gaupp *et al*. 1984, London 1990, Černý 1991a, b, Morteani *et al*. 2000), form the basis for the geochemical classification used to select pegmatites (1) to constrain the age of pegmatite emplacement with U–Pb dating and (2) to characterize the source of heterogeneous and homogeneous pegmatites and geochemically related granites with Pb isotopes.

Geological Setting of the Seridó Fold Belt

The Borborema Province is composed of three major tectonic zones: the Southern Domain, the Transversal Domain, and the Northern Domain (Archanjo 1993); these zones are separated by major east–west shear zones. The study area lies in the Northern Domain, within the Seridó transpressional fold belt, which is a shear zone that acted during the Brasiliano orogeny as a dextral strike-slip zone parallel to the folds (Corsini *et al*. 1991). The main direction of shearing is northeast–southwest, with east–west flexure to the south.

Two major Precambrian lithologies are recognized in the area: (1) the basement, including the Caicó Complex, and (2) the supracrustal rocks of the Seridó Group (Fig. 1). The Paleoproterozoic basement (partly the Caicó Complex) is composed of gneiss and migmatite designated as the Caicó magmatic suite (Legrand *et al*. 1991) and schist, quartzite, amphibolite, and marble known as the São Vicente Complex (Ebert & Claro 1970, Schobbenhaus 1984, Van Schmus *et al*. 1996). The Caicó Complex is a remnant of Paleoproterozoic crust formed around 2.2 Ga (De Souza *et al*. 1993).

The Seridó Group, composed of supracrustal rocks of Meso- to Neoproterozoic age, unconformably overlies the pre-Brasiliano Caicó Complex (Caby *et al*. 1995, Brito Neves *et al*. 2000). This group is divided into three formations, which are from bottom to top: the Jucurutú, the Equador, and the Seridó formations (Fig. 1; Jardim de Sá & Salim 1980, Jardim de Sá 1984). The Jucurutú Formation is constituted mainly of biotite gneiss. Interlayered carbonate- and calc-silicate-bearing horizons occur within the gneiss (Salim 1979, Jardim de Sá & Salim 1980). The Equador Formation is predominantly composed of muscovite-bearing quartzites. This formation contains polymictic metaconglomerate in the upper part of the lithostratigraphic section (Schobbenhaus 1984), whereas gneiss, schist, marble, and calc-silicate rocks are restricted to the top of the formation (Jardim de Sá & Salim 1980). The Seridó Formation is represented by aluminous metapelite with variable amounts of garnet, cordierite, staurolite, andalusite, and sillimanite. Interlayered quartz-, carbonate- and calc-silicate-bearing beds are also observed (Jardim de Sá & Salim 1980). This formation is interpreted by Jardim de Sá (1984) to be part of a synorogenic, turbiditic flysch-type sequence. The staurolite–andalusite and sillimanite zones in metapelites of the Seridó Formation indicate that the Seridó Group and the early Brasiliano intrusive rocks were metamorphosed to the upper-amphibolite-facies conditions during the Brasiliano cycle. The P–T estimates are 550°C and 0.20–0.25 MPa for the staurolite–andalusite zone and 600°C and 0.4 MPa for the sillimanite zone (Lima 1986, 1992, Corsini *et al*. 1998).

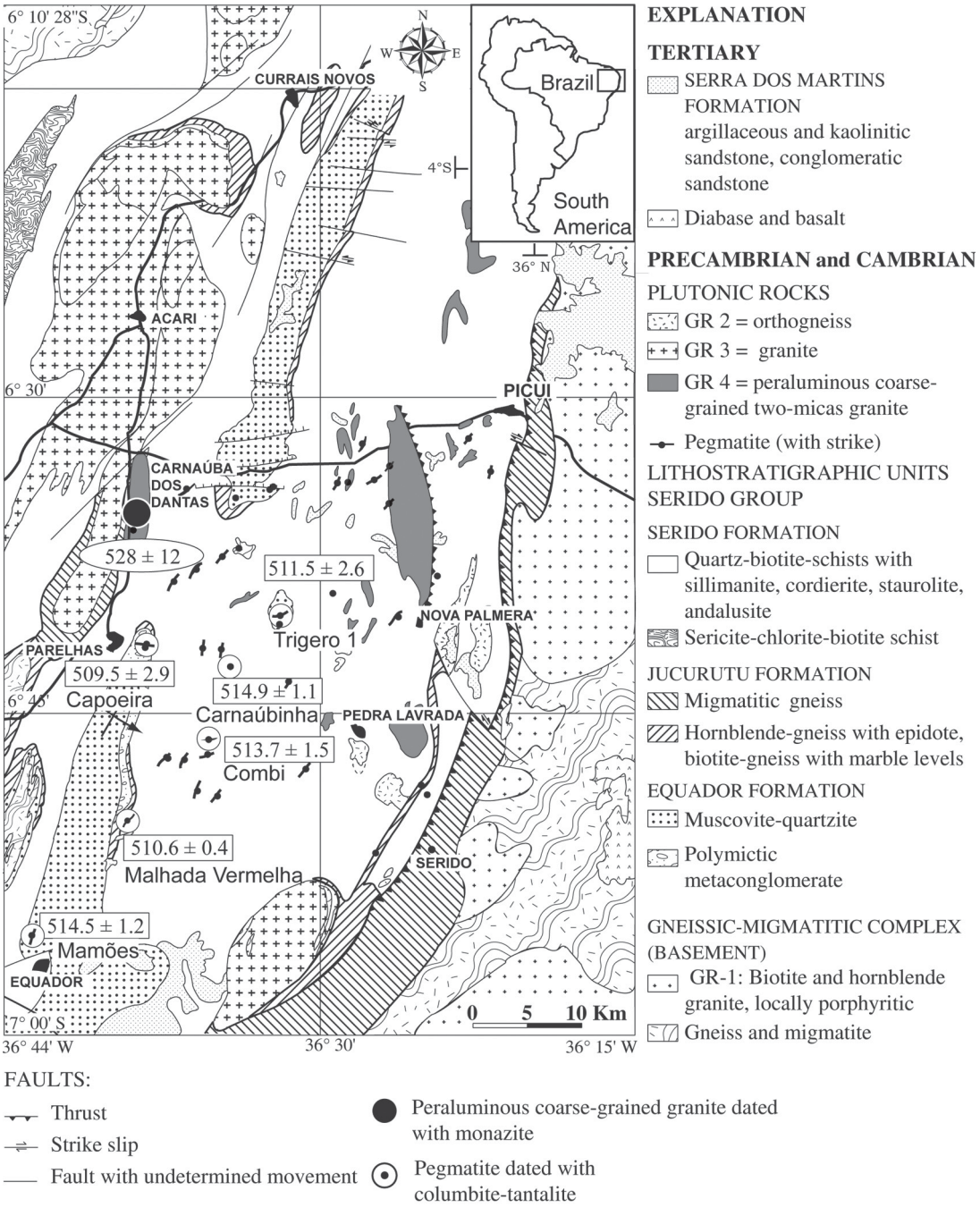

FIG. 1. Simplified geological map of the study area, modified after Lima (1980) and Da Silva (1993).

The Caicó Complex and the supracrustal sequence were intruded by different types of regionally widespread igneous rocks.

Late-Kinematic Pegmatites and Granites

In the study area, swarms of granitic pegmatite dykes and bodies intrude the supracrustal rocks. Individual pegmatite dykes and bodies generally strike northeast–southwest, which is approximately parallel to the direction of the fold system in the Seridó Belt (Fig. 1). A few pegmatites are east–west-striking. The orientation of the pegmatites indicates that the pegmatite-forming melts migrated along pre-existing structures during their ascent, in agreement with their late to post-tectonic setting, when NE–SW- and E–W-striking structures were reactivated under an extensional regime (Araújo *et al.* 2001).

The pegmatites are emplaced dominantly into the metapelites of the Seridó and quartzites of the Equador Formation (Fig. 1). The shape of the pegmatites ranges from vertical dykes (Fig. 2a) to lens-shaped bodies, with outcrop dimensions ranging from a few meters to several hundred meters in length and from a few meters up to one hundred meters in width (Fig. 2b). In the study area, economic pegmatites are generally lens-shaped and wider than a few meters, whereas barren pegmatites are predominantly vertical dykes that form distinct outcrops in the landscape owing to their resistance to weathering (Fig. 2a). Johnston (1945) reported that pegmatites from the Seridó fold belt display either a homogeneous or a heterogeneous internal mineral assemblage. On the basis of mineralogy and geochemistry (Baumgartner 2001), the heterogeneous pegmatites belong to the lithium – cesium – tantalum (LCT) type, which is characterized by elements such as Li, Rb, Cs, Be, Sn, Ga, and Ta, and subsidiary B, P, and F, and Ta > Nb (Ginsburg *et al.* 1979, Černý 1991b). The bulk mineralogical composition is granitic, with K-feldspar, albite, quartz, muscovite, and sporadic biotite. These minerals are typically present in both homogeneous and heterogeneous bodies. A great variety of accessory minerals, exceeding a hundred different species (Da Silva 1993), occur in the heterogeneous pegmatites. The characteristics and mineralogical assemblages are shown in Table 1.

The heterogeneous pegmatites are internally zoned, both mineralogically and texturally. The internal structure shows the following characteristics from the contact with the country rocks to the center of the pegmatite: 1) the border zone is commonly only a few centimeters wide. It contains abundant muscovite associated with quartz and some K-feldspar, displaying a comb texture. 2) The wall zone is compositionally and texturally similar to homogeneous pegmatites, with K-feldspar, albite, quartz, muscovite, and local biotite. The grain size increases toward the interior. K-feldspar contains perthite and shows a graphic intergrowth texture with quartz. Tourmaline and garnet are present in variable quantities. This zone is generally the thickest and is volumetrically the dominant part of the pegmatite. 3) The intermediate zone consists mainly of

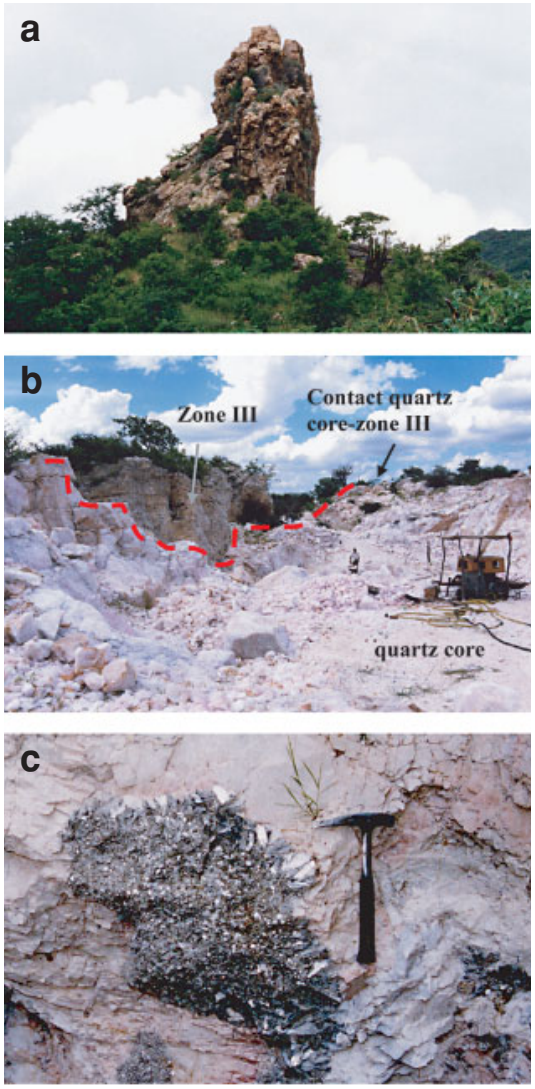

FIG. 2. a) Homogeneous pegmatite in the Seridó Belt. This type of pegmatite occurs as vertical dykes and is rarely of economical interest. b) Heterogeneous Feio pegmatite near Pedra Lavrada. It is lens-shaped, showing an extremely large quartz core (center) in contact with the intermediate zone (upper left side of picture). c) Pocket in a heterogeneous pegmatite. The pocket is composed of almost pure muscovite. The borders are coarse-grained, whereas the center is medium- to fine- grained (<1 cm). The pocket is hosted by pure K-feldspar of the intermediate zone.

large K-feldspar with rare quartz. 4) The core zone of the pegmatites is characterized by bodies of milky or pink quartz of variable size. Beryl, columbite–tantalite, and other accessory minerals grow from the border of the intermediate zone into the core zone. The size of the core varies among pegmatites from a few meters up to 50 m wide.

The transition between the wall into the intermediate zone can be either sharp or transitional. Individual crystals can reach dimensions over one meter with a weight of several tonnes. The volume of the crystals increases by two orders of magnitude from border to center, and the texture progresses from graphic K-feldspar and quartz intergrowths in the wall zone to large, euhedral crystals in the intermediate and the core zone. Muscovite pockets are abundant in the intermediate and core zones. Their size ranges from centimeters to decimeters. The pockets are generally round (Fig. 2c) and composed of muscovite with small amounts of K-feldspar, tourmaline, rare tabular columbite–tantalite and, locally, dark-green spinel (gahnite, $ZnAl_2O_4$). Muscovite forms centimeter-size sheets at the rim and millimeter-size flakes in the center of the pockets.

TABLE 1. MINERALOGY AND CHARACTERISTIC FEATURES OF THE PEGMATITES STUDIED IN THE SERIDÓ BELT, NORTHEASTERN BRAZIL

	Homogeneous	Heterogeneous			
		Border zone	Wall zone	Interm. zone	Core zone
Major minerals					
albite	+	+	+		
K- feldspar	+	+	+	+	
milky quartz	+	+	+		+
rose quartz					+
muscovite	+	+	+	pockets	
biotite	±		±		
Accessory minerals					
schorl	+	+	+		
beryl				+	
columbite–tantalite				+	
apatite			+		
elbaite				+	
spodumene				+	
petalite				+	
Textures					
graphic K-feldspar – quartz	+		+		
blocky				+	
Shape	dikes	---------- lenses ----------			
Size	width: < 10m length: < 500 m depth: ?	< 5 cm	from 1 m to several tens of meters		max 10 × 100 m
Orientation	NE-SW, EW or NS				
Host rock	metamorphic rocks of the Seridó Group				
Relationship pegmatite to wallrocks	concordant to discordant				

Pegmatites are emplaced in various host-rocks. The pegmatites of Mamões and Trigero I intrude quartzites from the Equador Formation, whereas the Capoeira pegmatite is emplaced in related metaconglomerates. The pegmatites Carnaúbinha, Combi, and Malhada Vermelha intrude the mica schists from the Seridó Formation (Fig. 1). The granitic rocks present in the region are classified into four groups, G1 to G4, based on their relationship with respect to structural elements (F1 to F4 and D1 to D4) and major tectonometamorphic events (Jardím de Sá *et al*. 1981). Syn- to late-D2 granitic rocks (G2 orthogneisses) yield an age of 1.9 Ga (Jardim de Sá 1994, Jardim de Sá *et al*. 1995), whereas G3 granites were emplaced at *ca*. 580 ± 30 Ma (dated on the Acari Batholith) during the deformation event D3 (Galindo *et al*. 1993, Jardim de Sá 1994, Legrand *et al*. 1991). The younger granites of groups G3 and G4 form large diapiric complexes (*e.g*., the Acari batholith) and minor intrusions, respectively. Group G4 granites (Fig.1) crop out as elongate bodies, cupolas, and stocks, forming numerous sills, discordant bulbous masses, and dykes (Da Silva 1993). The granites of group G4 have a peraluminous character, with muscovite, biotite, garnet, and accessory apatite, zircon, monazite, titanite, and tourmaline (Da Silva 1982, 1993). The emplacement of these granites shows a clear structural control. Jardim de Sá *et al*. (1981), Da Silva (1993), and Beurlen *et al*. (2001) linked the genesis of the regionally widespread pegmatites to the G4 granites, because of their close spatial relationship with those peraluminous granites, the locally pegmatitic texture of the granites, and the tight control by regional NE–SW- and E–W-striking lineaments on the distribution of both the pegmatites and the G4 granites. Intrusive rocks that are late- to post-Brasiliano orogeny show weak or no evidence for deformation and contain small amounts of xenoliths of supracrustal rocks (Souza Neto 1999).

Distribution of the pegmatite bodies

Bulk analyses of K-feldspar for trace elements have been made in order to characterize and classify the pegmatites (Baumgartner 2001). For heterogeneous pegmatites, a K/Rb *versus* Cs plot (Fig. 3) is used to discriminate the type of mineralization in granitic pegmatites. The Seridó pegmatites lie in the Be and Li–Be field, with some of the heterogeneous pegmatites falling in the Li–Cs–Be–Ta field. Homogeneous pegmatites are commonly barren. In Figure 4, homogeneous and heterogeneous pegmatites have been distinguished on a regional map. Using the economic potential of the heterogeneous pegmatites from Figure 3, a zonation can be observed. In fact, the Capoeira and Malhada Vermelha pegmatites show Li–Cs–Be–Ta phases. The pegmatites from the central part of the studied area contain Li–Be phases, and the ones from the eastern part contain Be phases. Several granitic plutons and intru-

sions are present in the Seridó belt (Fig. 4); attributing a parent pluton to the pegmatite field thus is difficult.

Analytical Methods

Chemical analyses were made at GeoForschungs-Zentrum (GFZ) Potsdam, Germany, using a Cameca SX 50 microprobe. Samples were prepared as polished thin sections. An operating voltage of 20 kV and a beam current of 40 nA were used for quantitative analysis. We monitored the elments Y, Sn, Sc, Bi, La, Ce, Pr, Nd, Th, and Pb, but concentrations are not reported as they are below or close to the detection limit.

The Pb isotope analyses of K-feldspar samples were carried out at the University of Geneva, Switzerland. Samples Peral 124, Cap 155, and Hu 063 were also leached and analyzed at GeoForschungsZentrum (GFZ) Potsdam, Germany. At Geneva, Pb isotope analyses were carried out on pre-leached K-feldspar from the pegmatites and the granites. K-feldspar from homogeneous and heterogeneous pegmatites, as well as granites, were separated by handpicking and crushed to a powder with an agate disk-mill. One mL of 14.4 M HNO_3 and 2 mL of 7 M HCl were added to the sample, which was placed on a hot plate at 180°C for more than 24 hours. The supernatant was discarded, and 1 mL of 14.4 M HNO_3 and 2 mL of concentrated HF were added to the residue in order to dissolve it. The sample was then placed on a hot plate at 180°C for 48 hours until it was completely digested. The solution was dried, and 3 mL of 14.4 M HNO_3 was added to the residue. The sample was placed on a hot plate at 180°C for 24 hours, and the solution was subsequently dried. A few drops of 4 M HBr was added to condition the sample. Lead was purified with anion exchange resins in an HBr medium. The procedural blanks were less than 120 pg Pb, which is insignificant in relation to the amount of lead encountered.

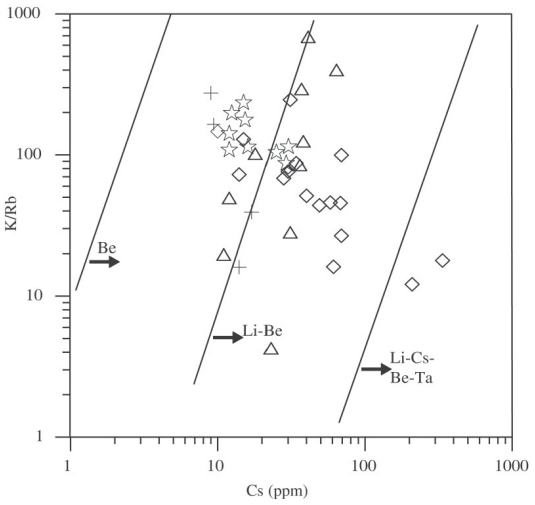

Fig. 3. K/Rb *versus* Cs plot of compositions of K-feldspar (after Černý 1989), and the link with the appearance of Be, Li–Be, and Li–Cs–Be–Ta phases. Heterogeneous pegmatites plot in the Li–Be and Li–Cs–Be–Ta field, indicating an economic potential for these pegmatites. Symbols: + coarse-grained peraluminous granite (G4), ☆ homogeneous pegmatites, Δ heterogeneous pegmatites (wall zone), ◇ heterogeneous pegmatites (intemediate zone).

The K-feldspar samples Peral 124, Cap 155, and Hu 063, analyzed at GFZ, Potsdam, Germany were leached in a mixture of HF:HBr = 1:20. Lead was separated using the HCl–HBr chemistry described in Romer *et al*. (2001). Total blank for these samples was less than 30 pg Pb.

Pb was loaded together with silica gel and H_3PO_4 on a single Re-filament and analyzed on MAT–Finnigan 262 mass spectrometers at the Department of Mineralogy of Geneva and at GFZ Potsdam. Mass fractionation was corrected with 0.08%/a.m.u. (Geneva) and 0.1%/a.m.u. (Potsdam) as determined from the repeated analyses of SRM–981. Replicate analyses of the SRM–981 standard were reproducible at the 2σ level within 0.05% for $^{206}Pb/^{204}Pb$, 0.08% for $^{207}Pb/^{204}Pb$, and 0.10% for $^{208}Pb/^{204}Pb$.

For U–Pb dating, individual columbite–tantalite crystals were crushed, and fragments showing fresh surfaces and a metallic luster were selected under a binocular microscope. All samples were leached before dissolution using the three-step procedure (20% HF, 6N HCl, and 7N HNO_3) of Romer & Smeds (1996). Leaching removes surface contamination, inclusions such as sulfides and K-feldspar, and most importantly dissolves metamict parts of columbite–tantalite (Fig. 5). Owing to unusually high contents of U and related damage of the crystal structure by α-recoil and fission tracks (Fig. 5; Romer 2003), some samples were strongly attacked during leaching with HCl and HNO_3 and developed brownish stains. These stains consisted of Fe-precipitates that may scavenge U and Pb differentially. Therefore, leached samples were separated a second time to include only grains with a metallic luster. Before dissolution, these samples were washed with 7 N HNO_3, distilled H_2O, and acetone. Samples were dissolved overnight with HF in Teflon beakers on a hot plate at 220°C. The dissolved samples were loaded in 3 N HCl on a column with AG1–X8 resin equilibrated in 3 N HCl. The column was rinsed with additional 3N HCl, and the U was eluted with 0.8 N HBr. The column was rinsed with 2 N HCl, and Pb was eluted with 6 N HCl. The earlier collected U was purified on the same column conditioned with 7 N HNO_3. The sample was rinsed with 7 N HNO_3 and 6 N HCl before the uranium was eluted with a 0.1 N HCl solution. Lead and uranium were loaded together with H_3PO_4 and silica gel on the same single Re-filament and analyzed at 1250 and 1350°C, respectively. Lead isotope ratios were corrected for fractionation with 0.1% /a.m.u. and lead contribution

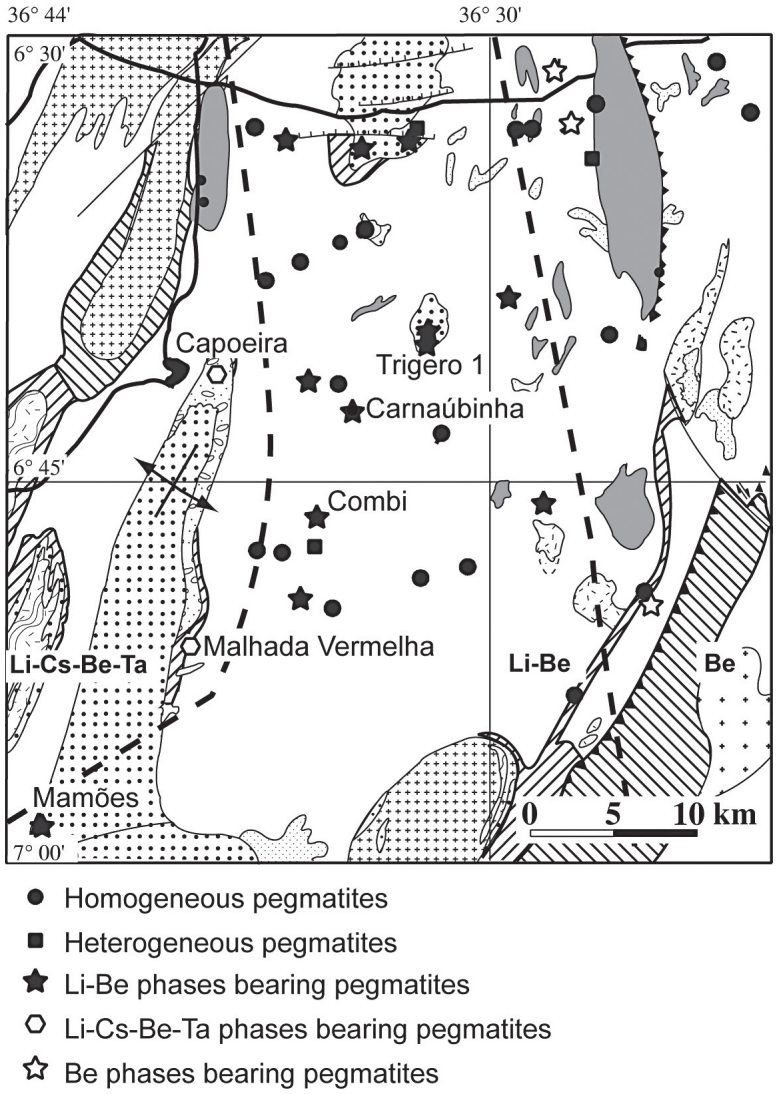

FIG. 4. Enlargement of Figure 1 showing the type of pegmatite. A spatial zoning is observed, from east (Be-bearing phases) to west (Li–Cs–Be–Ta enrichment). For lithology legend, see Figure 1.

from the isotopic tracer and blank. Uranium isotope ratios were corrected for fractionation with 0.1% /a.m.u. All samples were analyzed at GFZ Potsdam using a ^{205}Pb–^{235}U mixed isotope tracer. During the measurement period, total blanks were less than 15 pg for Pb and less than 1 pg for U.

RESULTS: PB ISOTOPES

The Pb isotopic composition of K-feldspar from the various pegmatites and the coarse-grained peraluminous granites spans a wide range in $^{206}Pb/^{204}Pb$ – $^{207}Pb/^{204}Pb$ and $^{206}Pb/^{204}Pb$ – $^{208}Pb/^{204}Pb$ diagrams (Figs. 6a, b) that

cannot be explained by *in situ* Pb-growth over the last 500 m.y. (the variation in $^{207}Pb/^{206}Pb$ is too large for the observed range in $^{206}Pb/^{204}Pb$ ratios). The range in isotopic compositions requires Pb derivation from several isotopically distinct reservoirs. Homogeneous pegmatites and the coarse-grained peraluminous granite (sample Peral 124, Figs. 6a, b) have distinctly more radiogenic Pb isotopic compositions than heterogeneous pegmatites (Table 2). The sample of peraluminous granite Peral 124 (Fig. 6b) yields the most radiogenic Pb, with a very high $^{207}Pb/^{204}Pb$ value. As most ^{207}Pb was formed during the early evolution of the Earth, such a high $^{207}Pb/^{204}Pb$ value can only be explained if the source of the granite acquired a high U/Pb more than 2 Ga ago. For a younger source, such a high $^{207}Pb/^{204}Pb$ could only be obtained at a much higher $^{206}Pb/^{204}Pb$ value than those of any of the samples in Figure 6 and Table 2. Thus, the Pb isotope data require the coarse-grained peraluminous granites be partially derived by melting of old continental crust. The isotopic heterogeneity among peraluminous coarse-grained granites (samples Peral 124 and 143, Figs. 6a, b) and homogeneous and heterogeneous pegmatites (Figs. 6a, b), suggests that the Pb source was highly heterogeneous or that the formation of these rocks involved mixing of Pb from different sources, characterized by different $^{207}Pb/^{204}Pb$ ratios. Lead with low $^{206}Pb/^{204}Pb$ and $^{207}Pb/^{204}Pb$ values was derived from a source with a low U:Pb ratio before it was contributed to the melt that formed the homogeneous pegmatites and peraluminous granites (Fig. 6b). The Pb isotopic compositions of the heterogeneous pegmatites fall along typical crustal Pb-growth curves (Fig. 6b).

Two samples of heterogeneous pegmatite clearly have distinctly higher $^{207}Pb/^{204}Pb$ values (samples Co 016 and Carn 160 in Fig. 6b). As these two samples are hosted by rocks different from those hosting the other heterogeneous pegmatites (Table 2), this contrast

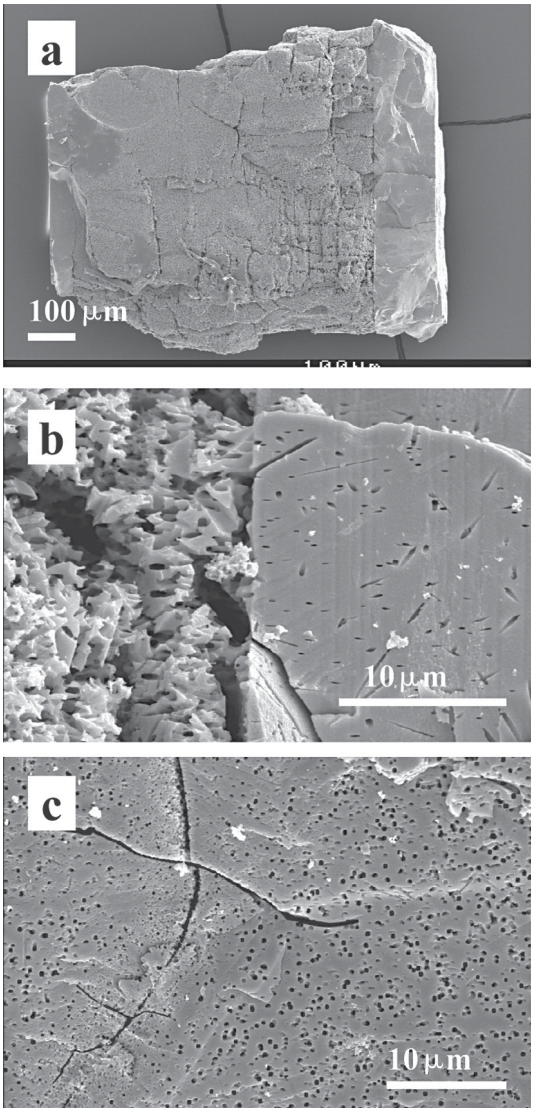

FIG. 5. SEM images of columbite–tantalite grains after leaching. a) Sample from the Carnaúbinha pegmatite. b) Enlargement of a). c) Sample from the Combi pegmatite. Note the etching of fission tracks, reflecting the distribution of U and, thus, indirectly also the distribution of damage induced by α-recoil in the crystal structure.

TABLE 2. Pb ISOTOPIC COMPOSITION OF K-FELDSPAR FROM GRANITES, HOMOGENEOUS AND HETEROGENEOUS (ZONE III) PEGMATITES OF THE SERIDÓ BELT

Type of rock	Host rock	Sample	$^{206}Pb/^{204}Pb^c$	$^{207}Pb/^{204}Pb^c$	$^{208}Pb/^{204}Pb^c$
[a] Gr	Seridó Fm. (qtz-bt schist)	Peral 124	19.958	16.217	39.863
[b] Gr	Seridó Fm. (qtz-bt schist)	Peral 124	19.930	16.170	39.654
[a] Gr	Seridó Fm. (qtz-bt schist)	Peral 143	18.445	15.589	37.954
[a]HoP	Seridó Fm. (qtz-bt schist)	Ho 042	19.181	15.656	38.288
[a]HoP	Seridó Fm. (qtz-bt schist)	Ho 224	19.622	15.844	39.260
[a]HoP	Seridó Fm. (qtz-bt schist)	Ho 263	19.354	15.765	38.213
[a]HeP	Seridó Fm. (qtz-bt schist)	Carn 160	18.532	15.745	38.606
[a]HeP	Equador Fm. (conglomerate)	Cap 155	18.149	15.503	38.788
[b]HeP	Equador Fm. (conglomerate)	Cap 155	17.800	15.502	37.844
[a]HeP	Seridó Fm. (qtz-bt schist)	Co 016	18.037	15.629	37.913
[a]HeP	Contact Seridó Fm./G2	Hu 063	16.695	15.370	36.777
[b]HeP	Contact Seridó Fm./G2	Hu 063	16.767	15.405	36.880
[a]HeP	Equador Fm. (conglomerate)	Ma 207	18.032	15.551	38.072
[a]HeP	Equador Fm. (quartzite)	Mamo 273	18.342	15.591	37.422
[a]HeP	Equador Fm. (quartzite)	Trig 235	18.686	15.588	38.069

[a] Samples analyzed at University of Geneva, Switzerland
[b] Samples analyzed at GFZ Potsdam, Germany
[c] Measured values corrected for mass fractionation with 0.1 %/a.m.u; reported values are reproducible to better than 0.1%.
Symbols: Gr: granite, HoP: homogeneous pegmatite, HeP: heterogeneous pegmatite.

in Pb isotopic composition likely reflects the influence of local host-rocks that were assimilated and contributed significantly to the Pb budget of the rare-element pegmatites.

Results: Columbite–Tantalite Composition and U–Pb Geochronology

The composition of the dated samples of columbite–tantalite falls in the ferrocolumbite and manganocolumbite fields (Table 3, Fig. 7). There is no significant incorporation of Sn, W, and Zr (with the notable exception of samples from Trigero and Carnaubinha, which are Zr-rich, Table 3). There are, however, important contributions of U and Ti. All samples contain variable amounts of UO_2 (between 0.05 to 3.68 wt%, Table 3), and these show a positive correlation with Ti as well as Ta/(Ta + Nb) (Fig. 8). This correlation of Ti and U in samples from the Trigero, Malhada Vermelha, and Mamões pegmatites may indicate the substitution of Ti and U for Nb and Ta, which seems to be favored at higher Ta contents. For each sample, there is little variation in the composition. Similar Ti-rich, Sn-poor columbite has been described from Weinebene, Austria, and was called titanian ferrocolumbite (Černý *et al.* 1989). The intimate intergrowth of this titanian ferrocolumbite with niobian rutile was interpreted to reflect the exsolution of rutile from a possibly orthorhombic precursor, such as titanian ixiolite (Černý *et al.* 1989). Abundant inclusions in the columbite–tantalite samples from the Trigero, Capoeira, and Mamões pegmatites (*e.g.,* Fig. 9a) may also reflect the exsolution of Ti–U-rich minerals, shifting the composition of these samples into the field of titanian columbite–tantalite. Generally, back-scattered-electron (BSE) images of the columbite–tantalite samples show no evidence of zoning, reflecting constant Ta/(Ta + Nb) values in individual grains. BSE images (Fig. 9a and c) show inclusions in

TABLE 3. REPRESENTATIVE ELECTRON-MICROPROBE DATA FOR COLUMBITE-TANTALITE MINERALS FROM GRANITIC PEGMATITES OF THE SERIDÓ BELT, NORTHEASTERN BRAZIL

	Malhada Vermelha		Combi		Mamões		Capoeira		Carnaubinha		Trigero 1	
Sample	Ma 206	Ma 206	Co 019	Co 019	Ma 279	Ma 279	Cap 203	Cap 203	Carn 158	Carn 158	Trig 245	Trig 245
MnO wt%	13.86	14.22	6.51	6.06	8.29	8.27	12.89	12.79	7.23	7.81	13.30	13.40
FeO	4.31	4.51	12.37	12.96	10.73	10.58	5.67	5.82	11.23	11.23	3.55	3.46
As_2O_3	0.64	0.00	0.27	0.11	0.03	0.00	0.00	0.25	0.35	0.00	0.03	0.07
Ta_2O_5	12.67	13.01	15.50	15.10	14.09	13.71	16.49	16.33	15.31	16.41	18.78	19.03
Nb_2O_5	63.73	65.42	64.31	64.31	63.33	63.85	58.01	58.12	62.84	62.02	53.41	53.49
WO_3	0.45	0.81	0.44	0.34	1.19	1.27	1.00	1.01	0.60	1.37	0.15	0.31
MgO	0.24	0.24	0.33	0.30	0.38	0.37	0.05	0.06	0.27	0.26	0.65	0.65
ZrO_2	0.272	0.282	0.000	0.000	0.038	0.058	0.459	0.520	0.373	0.020	0.522	0.514
CaO	0.190	0.027	0.003	0.000	0.014	0.019	0.002	0.008	0.060	0.005	0.004	0.000
TiO_2	2.20	1.83	1.09	1.09	2.23	2.14	4.05	4.14	1.81	1.67	5.58	5.71
UO_2	0.84	0.49	0.33	0.35	0.44	0.35	1.37	1.37	0.87	0.05	3.63	3.68
Total	99.56	100.99	101.22	100.71	100.86	100.83	100.12	100.49	100.98	101.00	99.72	100.38
Mn *apfu*	0.694	0.702	0.324	0.303	0.412	0.410	0.651	0.644	0.361	0.392	0.682	0.683
Fe	0.213	0.220	0.608	0.640	0.526	0.518	0.283	0.289	0.554	0.556	0.180	0.174
As	0.023	0.000	0.010	0.004	0.001	0.000	0.000	0.009	0.012	0.000	0.001	0.003
Ta	0.204	0.206	0.248	0.242	0.225	0.218	0.268	0.264	0.246	0.264	0.309	0.311
W	0.007	0.012	0.007	0.005	0.018	0.019	0.016	0.016	0.009	0.021	0.002	0.005
Mg	0.021	0.021	0.028	0.027	0.033	0.032	0.005	0.005	0.024	0.023	0.058	0.058
Zr	0.008	0.008	0.000	0.000	0.001	0.002	0.013	0.015	0.011	0.001	0.015	0.015
Ca	0.012	0.002	0.000	0.000	0.001	0.001	0.000	0.001	0.004	0.000	0.000	0.000
Ti	0.098	0.080	0.048	0.048	0.098	0.094	0.182	0.185	0.080	0.074	0.254	0.258
Nb	1.703	1.724	1.710	1.717	1.678	1.690	1.565	1.561	1.676	1.660	1.462	1.455
U	0.011	0.006	0.004	0.005	0.006	0.005	0.018	0.018	0.011	0.001	0.049	0.049
Total	2.997	2.985	2.990	2.994	3.002	2.994	3.005	3.010	2.990	2.995	3.016	3.014
Mn/(Mn + Fe)	0.765	0.761	0.348	0.321	0.439	0.442	0.697	0.690	0.395	0.414	0.791	0.797
Ta/(Ta + Nb)	0.107	0.107	0.127	0.124	0.118	0.114	0.146	0.145	0.128	0.137	0.174	0.176

The analytical data are recalculated on the basis of six atoms of oxygen and expressed in atoms per formula unit (*apfu*).

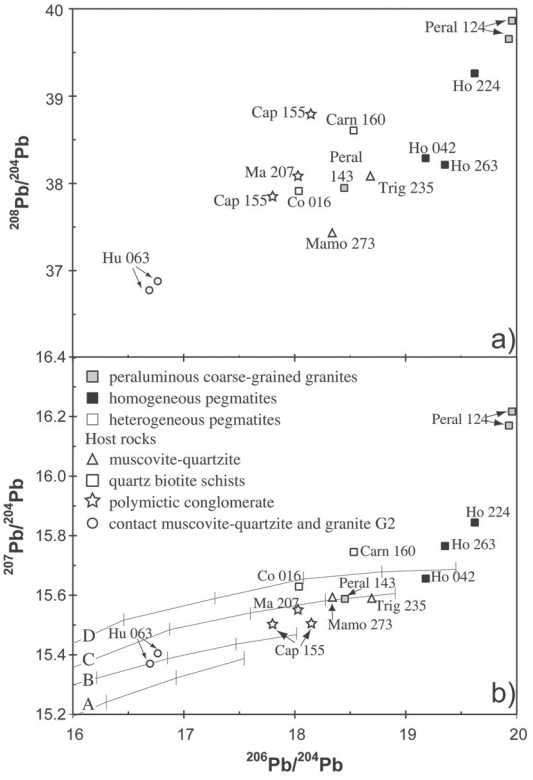

FIG. 6. a) Plots of a) $^{206}Pb/^{204}Pb$ *versus* $^{208}Pb/^{204}Pb$ and b) $^{206}Pb/^{204}Pb$ *versus* $^{207}Pb/^{204}Pb$ showing Pb isotopic compositions of K-feldspar from peraluminous granite, homogeneous, and heterogeneous pegmatites (intermediate zone). Lead-growth curves are from Zartmann & Doe (1981) and have been added for reference in b) (A: lower crust, B: mantle, C: orogen, D: upper crust).

some samples. The high content of uranium can produce damage in the crystal structure, eventually leading to partial or complete metamictization of the sample (Cesbron 1989), which favors the uptake of H_2O. The analyzed columbite–tantalite samples, however, contain less that 0.5 wt% H_2O. Metamictization permits redistribution of U and Pb and generally results in geochronologically open systems. The metamict parts of columbite–tantalite as well as inclusions of uraninite, once removed selectively by leaching (Fig. 5), have no influence on the age (Romer & Wright 1992, Smith *et al*. 2004). Incomplete removal or recrystallization of the columbite-group mineral, with incorporation of U and Pb in the recrystallized mineral, however, will result in excess scatter about the discordia (Romer 2003, Smith *et al*. 2004). Similarly disturbed U–Pb systematics with excess scatter about discordia lines are also obtained when exsolution results in the redistribution of U and Pb between exsolved zones and the host mineral. In the Seridó region, the ages of the pegmatites show no correlation with Ti or U concentrations of the columbite-group mineral.

Columbite–tantalite crystals were collected in the intermediate zone and on the border of the core zone from undeformed heterogeneous pegmatites at six different locations (Fig. 1). A monazite-group mineral (hereafter, monazite) from the coarse-grained peraluminous G4 granite has been sampled next to the road from Acari to Parelhas for purposes of radiometric dating (Fig. 1). The granite contains a similar mineralogical assemblage to the pegmatites, including muscovite, biotite, and garnet, and it is generally interpreted to be genetically related to the pegmatites (Jardim de Sá 1984, Da Silva 1993, Beurlen *et al*. 2001). Monazite and one sample of brabantite, rather than zircon, were dated from the granite sample to avoid any inheritance problem of zircon in this rock. The results of U–Pb dating are reported in Tables 4 and 5 and Figures 10 and 11.

The Malhada Vermelha pegmatite

A centimeter-large columbite–tantalite crystal from the intermediate zone was crushed to select five fragments. Electron-microprobe analyses (Table 3) show a manganocolumbite composition (Fig. 7), and BSE images reveal a near-homogeneous composition and few visible inclusions (Fig. 9b). The UO_2 and TiO_2 contents are high, from 0.49 to 0.84 wt% and 1.83 to 2.2 wt%, respectively (Table 3).

The five fragments define a good discordia, with a MSWD (mean squared weighted deviates) of 0.75 (Fig. 10a). The discordia intercepts the concordia at 510.6 ± 0.4 and 14 ± 19 Ma (2σ). Fraction 5 (Table 4) is strongly discordant, which is explained by recent lead loss or U–Pb fractionation during the leaching proce-

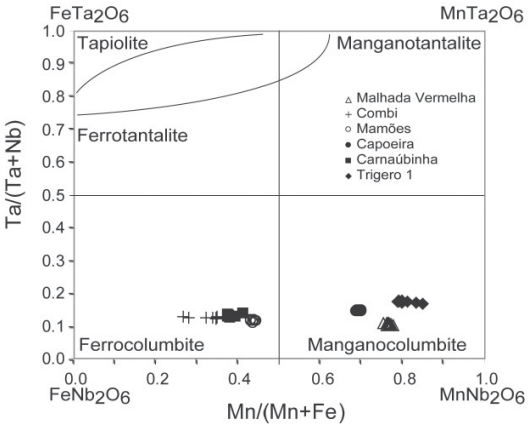

FIG. 7. Compositions of columbite–tantalite in pegmatites of the Seridó Belt.

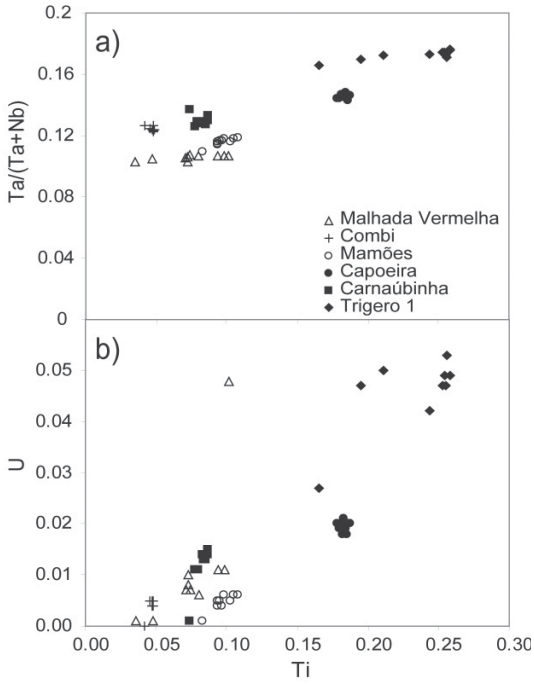

FIG. 8. Correlation of a) Ta/(Ta+Nb) *versus* Ti, and b) U *versus* Ti, showing the coupled substitution of U and Ti in columbite-group minerals.

dure. Fractions 1 to 3 are slightly reversely discordant, indicating U-loss. Uranium contents of the leached fractions range from 2740 to 8700 ppm (Table 4), and common lead contents vary from 0.24 to 4 ppm. The weighted average of apparent $^{207}Pb/^{206}Pb$ ages (Table 4) yields an age of 510.6 ± 0.4 Ma, which is in accordance with the U–Pb age.

The Combi pegmatite

Columbite–tantalite from this pegmatite is associated with K-feldspar and muscovite from the intermediate zone. The crystal habit is platy, differing from the one from Trigero 1 (see below). The electron-microprobe data plot within the ferrocolumbite field (Fig. 7, Table 3). Concentrations of UO_2 and TiO_2 (averages of

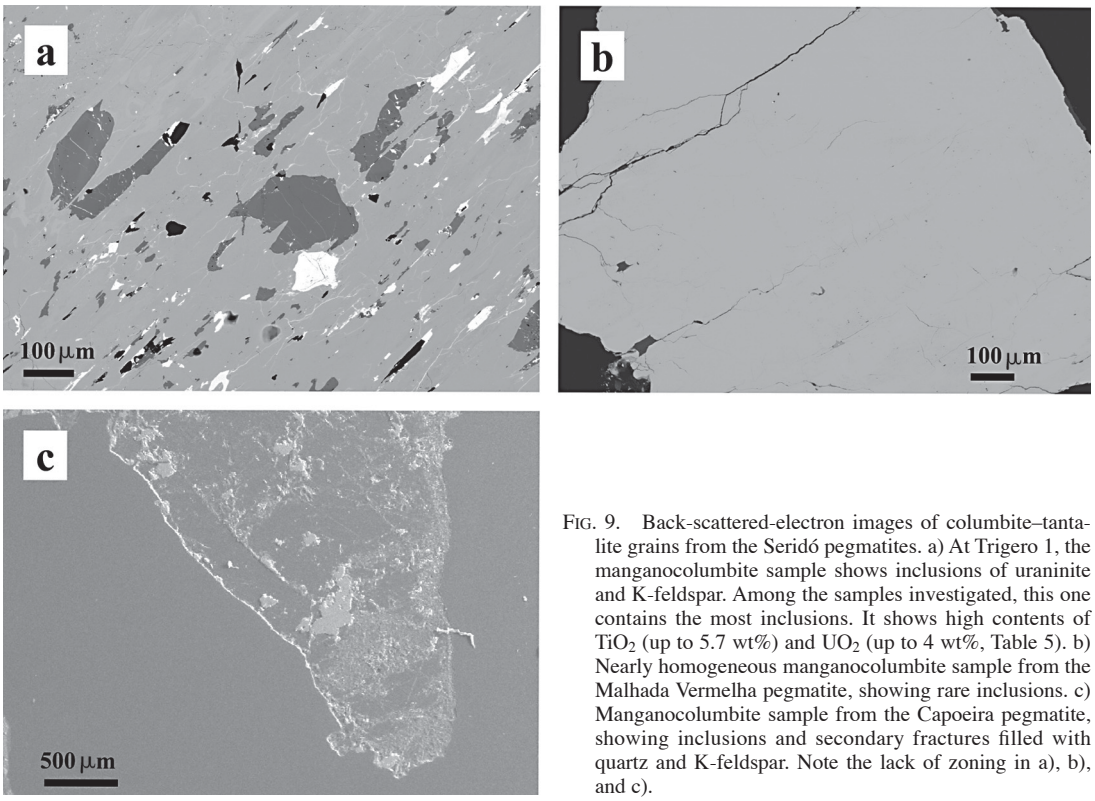

FIG. 9. Back-scattered-electron images of columbite–tantalite grains from the Seridó pegmatites. a) At Trigero 1, the manganocolumbite sample shows inclusions of uraninite and K-feldspar. Among the samples investigated, this one contains the most inclusions. It shows high contents of TiO_2 (up to 5.7 wt%) and UO_2 (up to 4 wt%, Table 5). b) Nearly homogeneous manganocolumbite sample from the Malhada Vermelha pegmatite, showing rare inclusions. c) Manganocolumbite sample from the Capoeira pegmatite, showing inclusions and secondary fractures filled with quartz and K-feldspar. Note the lack of zoning in a), b), and c).

TABLE 5. U–Pb ANALYTICAL RESULTS FOR COLUMBITE–TANTALITE IN GRANITIC PEGMATITES OF THE SERIDÓ REGION, NORTHEASTERN BRAZIL

Sample	Weight (mg)	Concentration (ppm)		$^{206}Pb/^{204}Pb$ M.R. [a]	Common lead (pg)	Radiogenic Pb (at.%) [b]			Th/U [d]	Atom ratios [c]			Apparent ages (Ma) [d]		
		U	Pb			^{206}Pb	^{207}Pb	^{208}Pb		$^{206}Pb/^{238}U$	$^{207}Pb/^{235}U$	$^{207}Pb/^{206}Pb$	$^{206}Pb/^{238}U$	$^{207}Pb/^{235}U$	$^{207}Pb/^{206}Pb$
Malhada Vermalha (a)															
1	0.049	6070	506	62000	12	94.47	5.43	0.10	0.0033	0.08292	0.65737	0.05750	514	513	511
2	0.057	6980	526	16210	113	94.46	5.43	0.11	0.0035	0.08242	0.65360	0.05713	511	511	511
3	0.074	7200	550	12280	216	94.46	5.43	0.10	0.0034	0.08354	0.66240	0.05751	517	516	511
4	0.086	2740	205	29510	26	94.50	5.43	0.07	0.0023	0.08184	0.64872	0.05749	507	508	510
5	0.161	8690	596	10160	644	94.47	5.43	0.11	0.0035	0.07484	0.59306	0.05747	465	473	510
Combi (b)															
6	0.020	1140	63.2	2231	24	94.51	5.44	0.05	0.0017	0.06010	0.47689	0.05755	376	396	513
7	0.040	830	56.5	2890	39	94.53	5.44	0.03	0.0011	0.07355	0.58360	0.05755	458	467	513
8	0.037	1270	91.2	7109	17	94.53	5.44	0.03	0.0010	0.07876	0.62540	0.05759	489	493	514
9	0.230	821	92.2	1989	58	94.56	5.42	0.02	0.0005	0.12018	0.94984	0.05732	732	678	504
10	0.042	1300	95.9	9753	13	94.53	5.44	0.03	0.0011	0.08090	0.64208	0.05757	502	504	513
11	0.035	851	58.4	3062	30	94.54	5.44	0.03	0.0010	0.07436	0.58955	0.05750	462	471	511
Mamoes (c)															
12	0.020	2210	170	5670	26	94.44	5.44	0.12	0.0040	0.08368	0.66498	0.05763	518	518	516
13	0.016	2320	172	3244	43	94.45	5.44	0.11	0.0037	0.08009	0.63585	0.05758	497	500	514
14	0.011	3610	267	4933	26	94.42	5.44	0.15	0.0048	0.08070	0.64093	0.05760	500	503	515
15	0.014	2530	187	5231	19	94.41	5.43	0.16	0.0051	0.08035	0.63750	0.05755	498	501	513
16	0.012	3730	240	3757	37	94.41	5.44	0.15	0.0051	0.06962	0.55267	0.05758	434	447	514
17	0.016	4210	220	4646	37	94.43	5.44	0.13	0.0042	0.05686	0.45149	0.05759	357	378	514
Capoeira (d)															
18	0.044	2730	1120	25430	120	94.42	5.41	0.17	0.0055	0.45115	3.56680	0.05734	2400	1542	505
19	0.060	1910	145	13490	30	94.44	5.43	0.13	0.0042	0.08298	0.65810	0.05752	514	514	512
20	0.042	1770	133	18870	6	94.45	5.43	0.12	0.0040	0.08260	0.65483	0.05750	512	511	511
21	0.086	1970	146	29740	14	94.44	5.44	0.14	0.0047	0.08144	0.64460	0.05740	505	505	507
22	0.120	1890	146	75220	2	94.44	5.43	0.14	0.0046	0.08496	0.67298	0.05745	526	523	509
23	0.082	2900	5.2	472	43	94.54	5.38	0.08	0.0027	0.00175	0.01375	0.05689	11	14	487
Carnaubinha (e)															
24	0.019	4700	365	18430	11	94.36	5.44	0.20	0.0067	0.08503	0.67548	0.05761	526	524	515
25	0.031	232	16.6	952	21	94.36	5.42	0.22	0.0071	0.07523	0.59618	0.05748	468	475	510
26	0.016	9160	842	1920	461	94.21	5.43	0.36	0.0119	0.09729	0.77287	0.05761	599	581	515
27	0.010	4590	344	7750	15	94.39	5.44	0.17	0.0057	0.08206	0.65174	0.05760	508	510	515
28	0.035	3240	322	1390	532	94.16	5.43	0.41	0.0136	0.10381	0.82519	0.05765	637	611	517
Trigero 1 (f)															
29	0.055	7280	578	14450	138	94.55	5.43	0.02	0.0007	0.08699	0.68938	0.05748	538	532	510
30	0.080	5870	459	27360	94	94.55	5.43	0.02	0.0007	0.08568	0.67865	0.05745	530	526	509
31	0.029	14730	1117	87350	26	94.54	5.44	0.03	0.0008	0.08330	0.66088	0.05754	516	515	512
32	0.066	8640	689	34140	94	94.54	5.44	0.02	0.0008	0.08759	0.69483	0.05754	541	536	512
33	0.035	15200	1152	110010	26	94.55	5.43	0.02	0.0007	0.08332	0.65997	0.05745	516	515	509
34	0.024	17430	1290	96840	22	94.54	5.44	0.02	0.0007	0.08137	0.64588	0.05757	504	506	513

[a] Measured ratios (M.R.) of the lead isotopes corrected for fractionation, with 0.1% /a.m.u. and lead contribution from the isotopic tracer. All samples were analyzed at GFZ (GeoForschungsZentrum), Potsdam, Germany, using a ^{205}Pb–^{235}U mixed isotopic tracer. Analytical details are given in Romer & Smeds (1996). During the measurement period, total blanks were less than 15 pg for lead and less than 1 pg for uranium.

[b] Lead corrected for fractionation, blank, isotopic tracer, and initial lead ($^{206}Pb/^{204}Pb$ = 18.8, $^{207}Pb/^{204}Pb$ = 15.7, $^{208}Pb/^{204}Pb$ = 38.4).

[c] Th/U calculated from radiogenic $^{208}Pb/^{206}Pb$ and age of the sample.

[d] Apparent ages were calculated using the constants of Jaffey *et al.* (1971) recommended by IUGS (Steiger & Jäger 1977).

0.3 and 1.09 wt%, respectively) are relatively high and favor metamictization of the minerals (Table 3).

The six fractions define a discordia with a MSWD of 1.04, an upper intercept age at 513.7 ± 1.5 Ma and a lower intercept at 7 ± 15 Ma (2σ) (Fig. 10b). Fraction 6 is strongly discordant owing to lead loss. Fraction 9 is markedly reversely discordant and has an anomalously young $^{207}Pb/^{206}Pb$ age if compared to the other fractions of the same crystal (Table 4). This anomalous $^{207}Pb/^{206}Pb$ age may reflect U and Pb fractionation during partial recrystallization of the metamict columbite–tantalite, which eventually prevents the complete removal of U and Pb from the strongly damaged, potentially open parts of the mineral (*cf.* Romer 2003, Smith *et al.* 2004). Therefore, fraction 9 is not included in the calculation of the age. The weighted average of apparent $^{207}Pb/^{206}Pb$ ages (Table 4) corresponds to an age of 513.7 ± 1.0 Ma. Uranium concentrations vary from 830 to 1300 ppm in the samples, and the common lead content ranges from 0.3 to 2.5 ppm.

The Mamões pegmatite

Columbite–tantalite was collected at the border of the core zone, and is associated with K-feldspar. Electron-microprobe analyses plot within the ferrocolumbite field near the border of the manganocolumbite field (Table 3, Fig. 7). The UO_2 and TiO_2 contents range from 0.35 to 0.44 wt% and from 2.14 to 2.23 wt%, respectively (Table 3).

Among the six fractions from Mamões, one fraction is concordant (12, Table 4), three fractions are subconcordant (13, 14 and 15, Table 4), and two fractions are strongly discordant (16 and 17, Table 4). They define a discordia that yields intercepts at 514.5 ± 1.2 Ma and 1.3 ± 6.3 Ma (2σ) and a MSWD of 0.25 (Fig. 10c). The contents of U and common Pb vary respectively from 2210 to 4210 ppm and from 1.3 to 3.1 ppm (Table 4).

The Capoeira pegmatite

The selected crystal comes from a transitional zone between the intermediate and core zones. Bladed albite and quartz are associated with the columbite–tantalite, as well as large sheets (< 10 cm) of muscovite. Electron-microprobe data plot in the manganocolumbite field (Fig. 7, Table 3), and BSE images show abundant inclusions. The most widespread are uraninite, K-feldspar, and an unidentified metamict mineral (Fig. 9c). Average concentrations are 1.37 wt% for UO_2 and 4.1 wt% for TiO_2 (Table 3).

Six columbite–tantalite fragments were analyzed, and yield discordant data-points in Figure 10d. Fragments 18 and 23 (Table 4) are responsible for most of the scatter about the discordia (Fig. 10d). Fraction 23 was included in the calculation of the discordia, whereas the strongly reversely discordant fraction 18 has been omitted, as it contributed most of the excess scatter. The five fractions yield an upper intercept age at 509.5 ± 2.9 Ma and a lower intercept at 0.6 ± 1.4 Ma (2σ), for a discordia with a MSWD of 12. Uranium contents vary between 1770 and 2900 ppm, whereas concentrations of common lead are between 0.02 to 0.7 ppm (Table 4). This sample has the highest U content in the structure of the columbite–tantalite mineral and, therefore, has also accumulated the highest amount of

TABLE 5. U–Pb ANALYTICAL RESULTS FOR MONAZITE AND BRABANTITE FROM A GRANITE IN THE SERIDÓ REGION, NORTHEASTERN BRAZIL

Sample [a]	Weight (mg)	Concentration (ppm)		$^{206}Pb/^{204}Pb$ M.R. [b]	Common lead (pg)	Radiogenic Pb (at.%) [b]			Th / U [d]	Atom ratios [c]			Apparent ages (Ma) [e]		
		U	Pb			^{206}Pb	^{207}Pb	^{208}Pb		$^{206}Pb/^{238}U$	$^{207}Pb/^{235}U$	$^{207}Pb/^{206}Pb$	$^{206}Pb/^{238}U$	$^{207}Pb/^{235}U$	$^{207}Pb/^{206}Pb$
35 (Brb)[f]	0.004	17100	2550	373.9	200	10.91	0.63	88.46	26.1	0.01831	0.14551	0.05763	117	138	516
36 (Mnz+Xnt)	0.006	4775	298	197.6	430	78.07	4.52	17.41	0.71	0.04229	0.33766	0.05790	267	295	526
37 (Mnz)	0.052	3610	2580	1170	860	10.27	0.60	89.13	28.0	0.08408	0.67423	0.05816	520	523	536
38 (Mnz)	0.029	5560	2850	87.97	7940	9.85	0.58	89.57	29.3	0.05243	0.42479	0.05877	329	360	558
39 (mo)	0.036	4240	3000	336.4	2600	10.61	0.61	88.78	27.0	0.08448	0.67266	0.05775	523	522	520
40 (mo)	0.045	3490	2490	913.4	890	9.88	0.57	89.55	29.2	0.08049	0.64282	0.05792	499	504	527

[a] Small grains of monazite (Mnz) were selected for analyses. One grain contained xenotime (Xnt).
[b] Measured ratios (M.R.) of the lead isotopes corrected for fractionation, with 0.1% / a.m.u., and lead contribution from the isotopic tracer. All samples were analyzed at GFZ (GeoForschungsZentrum), Potsdam, Germany, using a $^{205}Pb–^{235}U$ mixed isotopic tracer.
[c] Lead corrected for fractionation, blank, isotopic tracer, and initial lead ($^{206}Pb/^{204}Pb = 20.0 \pm 0.1$, $^{207}Pb/^{204}Pb = 16.22 \pm 0.03$, $^{208}Pb/^{204}Pb = 39.9 \pm 0.2$).
[d] Th/U calculated from radiogenic $^{208}Pb/^{206}Pb$ and age of the sample.
[e] Apparent ages were calculated using the constants of Jaffey *et al.* (1971) recommended by IUGS (Steiger & Jäger 1977).
[f] Brabantite [$CaTh(PO_4)_2$, symbol Brb]: Th contents of 45–50% were calculated from $^{208}Pb_{Brb} / ^{204}Pb_{Brb}$.

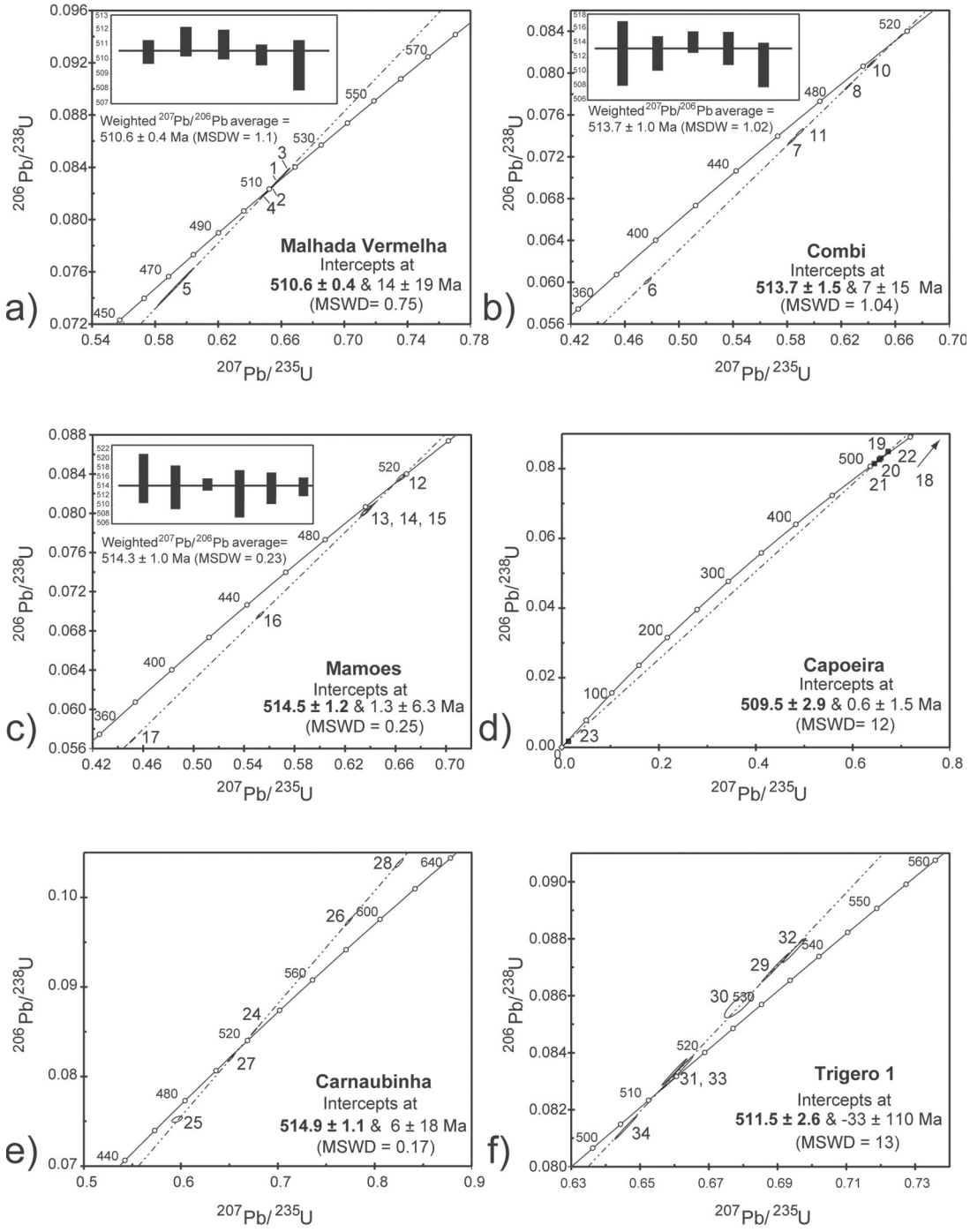

FIG. 10. Concordia diagrams for columbite–tantalite samples from rare-element-enriched pegmatites of northeastern Brazil. Intercepts and 2σ uncertainties were calculated using a program by Ludwig (1999). In (d), squares are shown instead of error ellipses because these are too small to be shown at the scale of the concordia.

structural damage due to the radioactive decay of U and its unstable daughter isotopes. Thus, this columbite–tantalite sample may have the highest potential for redistribution of U and Pb, which may also explain the excess scatter of the data (MSWD = 12), if there had been partial recrystallization after U and Pb migration (*cf.* Romer 2003).

The Carnaúbinha pegmatite

The columbite–tantalite from this pegmatite is intergrown with K-feldspar and muscovite. The electron-microprobe data plot in the ferrocolumbite field (Fig. 7, Table 3). They show relatively high amounts of UO_2 (0.87 wt%) and TiO_2 (1.8 wt%, Table 3).

Five fragments from a single crystal were selected. Fractions 25 and 27 are discordant, and fractions 24, 26, and 28 are reversely discordant (Fig. 10e). A discordia with a MSWD of 0.17 yielding intercepts at 514.9 ± 1.1 and 6 ± 18 Ma (2σ) is obtained if fraction 25 is omitted. Concentrations of lead are the highest among all fractions of the Seridó columbite–tantalite (0.5 to 40 ppm), and uranium concentrations range from 250 to 9200 ppm (Table 4).

The Trigero 1 pegmatite

In the intermediate zone of this pegmatite, columbite–tantalite is intimately associated with microcline. The electron-microprobe data plot in the manganocolumbite field (Fig. 7, Table 3), and BSE images show abundant inclusions. Uraninite, K-feldspar, and copper sulfides are the most common inclusions, but an unidentified U-rich mineral also is present (Fig. 9a). Average UO_2 and TiO_2 contents are 3.65 and 5.6 wt%, respectively (Table 3).

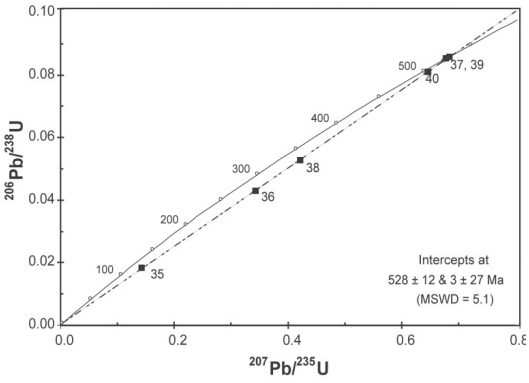

FIG. 11. Concordia diagram for monazite samples from the coarse-grained peraluminous G4 granite. Intercepts and 2σ uncertainties were calculated with the program of Ludwig (1999). Squares are shown instead of error ellipses because these are too small to be visible at scale of the diagram.

Six fragments from a single crystal were analyzed. The six columbite–tantalite fragments define a discordia with a MSWD of 13, an upper intercept at 511.5 ± 2.6 Ma and a lower intercept at –33 ± 110 Ma (2σ) (Fig. 10f). Fractions 29, 30 and 32 are reversely discordant. This columbite–tantalite sample is characterized by high contents of U (5800 to 17430 ppm) that are related to inclusions of uraninite. Contents of common lead vary from 0.7 to 2.5 ppm (Table 4).

The coarse-grained peraluminous granite

Five fractions of a crystal of monazite and one of brabantite [$CaTh(PO_4)_2$] from the G4 granite were analyzed (anal. 35–40, Table 5). One grain of monazite (sample 36) is intergrown with xenotime (YPO_4). The data yielded by the brabantite sample do not differ from those of the monazite samples (Table 5). There is significant excess scatter in the data. This scatter is related to sample 38 (not shown on the concordia diagram in Fig. 11), which has a distinctly lower $^{206}Pb/^{204}Pb$ ratio than the other samples, and to sample 39, which has a distinctly lower $^{207}Pb/^{206}Pb$ ratio than the other subconcordant samples (Fig. 11). Using the Pb isotopic composition of the granite sample Peral 124 ($^{207}Pb/^{204}Pb$ = 16.2, Table 2) for the common Pb correction, the data yield a discordia with intercepts at 528 ± 12 and –3 ± 27 Ma (Fig. 11). The upper intercept age of the discordia is sensitive to the common Pb correction. Using a common Pb with a lower $^{207}Pb/^{204}Pb$ ratio than the one deduced from sample Peral 124 results in older intercept ages. Therefore, whatever the common Pb correction, the youngest age yielded by the data for the coarse-grained peraluminous granite G4 remains older than the oldest pegmatite dated in this study. Because of the large uncertainty, 12 m.y., associated with the age of the coarse-grained peraluminous granite G4, it remains open to question whether this granite is only slightly older (528 Ma –12 m.y. = 516 Ma) or significantly older (528 Ma + 12 m.y. = 540 Ma) than the heterogeneous pegmatites.

DISCUSSION

Composition of columbite–tantalite and age of emplacement of the pegmatites

Samples of columbite–tantalite from the heterogeneous pegmatites in the Seridó Belt have a composition between ferrocolumbite (Combi, Carnaúbinha, and Mamões pegmatite) and manganocolumbite (Capoeira, Malhada Vermelha, and Trigero 1 pegmatite) (Fig. 7). Among the numerous elements known to be accommodated in columbite–tantalite minerals, Ti and U are the most important. Only in two samples are there significant amounts of Zr (Trigero and Carnaubinha; Table 3).

Columbite–tantalite-bearing pegmatites in the study area yield ages that are restricted to a narrow range between 509.5 ± 2.9 Ma and 514.9 ± 1.1 Ma (Fig. 10), indicating that their formation was roughly coeval. These ages are the first U–Pb ages on columbite–tantalite in the Seridó region. Previously, 450 and 550 Ma Rb–Sr ages on muscovite and a single U–Pb age on uraninite, 780 Ma, had been reported by Agrawal (1986). Our ages indicate a shorter time-frame of emplacement during the end of the Brasiliano orogeny than the earlier data. The new data are in accordance with the structural work by Araújo *et al*. (2001) in the Seridó Belt. The age variation among the pegmatites does not show any relationship to pegmatite orientation or with host rock, but instead seems to correlate with the degree of evolution. The youngest pegmatites, including Capoeira and Malhada Vermelha (509.5 ± 2.9 and 510.6 ± 0.4 Ma, respectively), show the most evolved mineralogy, with an economic potential defined by Li–Cs–Be–Ta phases.

Relationship between coarse-grained granites and pegmatites

According to Černý (1991b), the granitic intrusions genetically associated with pegmatites are typically located in the center of the pegmatite group. The parental granite of a pegmatite group can be either exposed or hidden, depending on the depth of erosion. In some regions, the parental granite is well exposed, such as the Osis Lake granite, southeastern Manitoba, Canada, (Černý 1991b) or is believed to be hidden, such as in the Sveconorwegian terranes, where the pegmatites studied are older than the granite exposed at the same erosional level (Romer & Smeds 1996). In the Seridó region, owing to the large uncertainty in the age of the coarse-grained peraluminous granite, we can only conclude that this granite is older than the pegmatites. Granites with the same mineralogical and geochemical signatures as the peraluminous granite dated, however, could have been a possible parental granitic melt for the rare-element pegmatites.

Pb isotopic composition of the pegmatites and the peraluminous granite

The Pb isotopic variation of K-feldspar from the rocks of this study seems to reflect Pb contribution of local assimilation of host-rocks. The scatter of the data can be explained by the variation of the composition of the immediate host-rocks (Fig. 6). Country rocks range from muscovite quartzite and quartz biotite schist to polymictic conglomerate. Sample Hu 063, which has low isotopic values, occurs in a pegmatite located at the contact between muscovite quartzite and a G2 granite (Fig. 6, Table 2).

Sample Peral 124 has Pb high isotopic values and is similar to the isotopic composition of old continental crust (Fig. 6, high U/Pb, > 2Ga). This sample has the highest $^{207}Pb/^{204}Pb$ value of all samples occurring in pegmatites hosted by quartz–biotite schist.

We suggest that several separate batches of magma were responsible for the formation of the pegmatites. Host rocks with geochemically and isotopically distinct characteristics have contributed in variable amounts to these batches of magma, as reflected in the Pb isotopic compositions of K-feldspar.

Conclusions

(1) The LCT-type granitic pegmatites from the Seridó fold belt are spatially related to coarse-grained peraluminous granites in this belt. A zoning based on the economic potential is observed, with Be-bearing phases noted in pegmatites on the eastern side of the study area, whereas pegmatites bearing Li–Cs–Be–Ta phases are present in the western part.

(2) U–Pb dating of manganocolumbite and ferrocolumbite reveal ages between 509.5 ± 2.9 Ma and 514.9 ± 1.1 Ma for the heterogeneous pegmatites. One coarse-grained peraluminous granite sample yields an age of 528 ± 12 Ma. Thus, the pegmatites are younger than this granite. The U–Pb ages and the absence of deformation in the heterogeneous pegmatites imply that they are late- to post-tectonic, and that the ages of 509.5 ± 2.9 Ma and 514.9 ± 1.1 Ma bracket the end of the Brasiliano orogeny in this region. At the end of this orogeny, the compressional tectonic setting changed to an extensional regime, and ductile deformation changed to brittle deformation. This permitted formation of evolved melts and their ascent along pre-existing NE–SW structures.

(3) Lead isotope data from K-feldspar from the coarse-grained peraluminous granite, as well as homogeneous and heterogeneous pegmatites, show a correlation between $^{207}Pb/^{204}Pb$ and the host rocks of the pegmatites. These results suggest that the magmas, emplaced in several batches, were modified by addition of Pb by assimilation of the isotopically distinct host-rocks.

(4) The peraluminous granite that we dated does not seem to be the parent pluton; thus, other granites in the Seridó region should be investigated geochemically and geochronologically to determine the genetic relationship between the outcropping granites and the homogeneous and heterogeneous pegmatites.

Acknowledgements

This fieldwork was supported by the commission of the Swiss Academy of Sciences (ASSN) and by a Society of Economic Geologists (SEG) Hugh E. McKinstry student Grant 2000. Financial contribution also comes from the Swiss National Science Foundation (Grants 20–47.260.96 and 2000–062000.00/1). Thanks to Eric Reusser (ETH Zürich) for the BSE images. We

thank Dieter Rhede and Oona Appelt (GFZ Potsdam) for carrying out the electron-microprobe analyses of the columbite samples. Urs Schaltegger (University of Geneva, Switzerland) is thanked for his constructive discussions and suggestions that meaningfully improved the manuscript. The thorough and constructive reviews by W.B. Simmons and K. Webber helped greatly.

REFERENCES

AGRAWAL, V.N. (1986): Structural evidence for an early episode of pegmatite emplacement in the Seridó Group. *In* 12th Simp. Geol. Nordeste. *Soc. Bras. Geol.*, 282-289 (abstr.).

ARAÚJO, M.N.C., ALVES DA SILVA, F.C. & JARDIM DE SÀ, E.F. (2001): Pegmatite emplacement in the Seridó Belt, northeastern Brazil: late stage kinematics of the Brasiliano orogen. *Gondwana Res.* **4**(1), 75-85.

ARCHANJO, C.J. (1993): *Fabrique de plutons granitiques et déformation crustale du nord-est du Brésil*. Thèse de doctorat, Univ. de Toulouse III, Toulouse, France.

BAUMGARTNER, R. (2001): *Genèse des pegmatites à colombo-tantalite et béryl de la province pegmatitique Seridó* (*Rio Grande do Norte, Brésil*). Thèse de maîtrise, Univ. de Genève, Genève, Suisse.

BEURLEN, H. (1995): The mineral resources of the Borborema Province in northeastern Brazil and its sedimentary cover: a review. *J. S. Am. Earth Sci.* **8**, 365-376.

BEURLEN, H., DA SILVA, M.R.R. & DE CASTRO, C. (2001): Fluid inclusion microthermometry in Be–Ta–(Li–Sn)-bearing pegmatites from the Borborema Province, northeast Brazil. *Chem. Geol.* **173**, 107-123.

BEUS, A.A. (1966): Distribution of tantalum and niobium in muscovites from granitic pegmatites. *Geokhimiya* **10**, 1216-1220 (in Russ.).

BRITO NEVES, B.B., DOS SANTOS, E.J. & VAN SCHMUS, W.R. (2000): Tectonic history of the Borborema Province, northeastern Brazil. *In* Tectonic Evolution of South America (U. Cordani, E.J. Milani, A. Thomaz Filho & D.A. Campos, eds.). *Proc. Int. Geol. Congress, 31st* (Rio de Janeiro), 151-182.

CABY, R., ARTHAUD, M.H. & ARCHANJO, C.J. (1995): Lithostratigraphy and petrostructural characterization of supracrustal units in the Brasiliano Belt of northeast Brazil: geodynamic implications. *J. S. Am. Earth Sci.* **8**, 235-246.

ČERNÝ, P. (1991a): Rare-element granitic pegmatites. I. Anatomy and internal evolution of pegmatite deposits. *Geosci. Canada* **18**, 49-67.

ČERNÝ, P. (1991b): Rare-element granitic pegmatites. II. Regional to global environments and petrogenesis. *Geosci. Canada* **18**, 68-81.

ČERNÝ, P. (1989): Characteristics of pegmatite deposits of tantalum. *In* Lanthanides, Tantalum and Niobium (P. Möller, P. Černý & F. Saupé, eds.). Springer, Berlin, Germany (195-239).

ČERNÝ, P., CHAPMAN, R., GÖD, R., NIEDERMAYR, G. & WISE, M.A. (1989): Exsolution intergrowth of titanian ferrocolumbite and niobian rutile from the Weinebene spodumene pegmatites, Carinthia, Austria. *Mineral. Petrol.* **40**, 197-206.

CESBRON, F.P. (1989): Mineralogy of the rare-earth elements. *In* Lanthanides, Tantalum and Niobium (P. Möller, P. Černý & F. Saupé, eds.). Springer, Berlin, Germany (3-26).

CORSINI, M., LAMBERT DE FIGUEIREDO, L., CABY, R., FRÉRAUD, G., RUFFET, G. & VAUCHEZ, A. (1998): Thermal history of the Pan-African/Brasiliano Borborema Province of northeast Brazil deduced from Ar^{40}/Ar^{39} analysis. *Tectonophysics* **285**, 103-117.

CORSINI, M., VAUCHEZ, A., ARCHANJO, C.J. & JARDIM DE SÁ, E.F. (1991): Strain transfer at continental scale from a transcurrent shear zone to a transpressional fold belt: the Patos–Seridó System, northeastern Brazil. *Geology* **19**, 586-589.

DA SILVA, M.R.R. (1982): *Petrologia e geochimica de pegmatitos de região de Picui-Pedra Lavrada* (*PB*). M.Sc. thesis, Univ. Federal. Pernambuco, Recife, Brazil.

DA SILVA, M.R.R. (1993): *Petrographical and Geochemical Investigations of Pegmatites in the Borborema Province of Northeastern Brazil*. Ph.D. thesis, Univ. of München, München, Germany.

DA SILVA, M.R.R., HÖLL, R. & BEURLEN, H. (1995): Borborema pegmatitic province: geological and geochemical characteristics. *J. S. Am. Earth Sci.* **8**, 355-364.

DE SOUZA, Z.S., MARTIN, H., MACEDO, M.H.F., PEUCAT, J.J. & JARDIM DE SÁ, E.F. (1993): Un segment de croûte continentale juvénile d'âge protérozoïque inférieur: le complexe de Caicó (Rio Grande do Norte, NE-Brésil). *C.R. Acad. Sci.* **316**, 201-208.

EBERT, H. & CLARO, R. (1970): The Precambrian geology of the "Borborema" belt (states of Paraiba and Rio Grande do Norte, northeastern Brazil) and the origin of its mineral provinces. *Geol. Rundschau* **59**, 1292-1326.

GALINDO, A.C., DALL'AGNOL, R., MCREATH, I. & SHELLER, T. (1993): Geochronologia dos granitoídes brasilianos da região de Caraúbas–Umarizal, Oeste do Rio Grande do Norte. 15th Simp. Geol. Nordeste. *Soc. Bras. Geol., Actas* **1**, 325-328.

GAUPP, R., MÖLLER, P. & MORTEANI, G. (1984): *Tantal-pegmatite; Geologische, Petrologische und Geochemische Untersuchungen*. Bornträger, Berlin, Germany (124).

GINSBURG, A.I., TIMOFEYEV, I.N. & FELDMAN, L.G. (1979): *Principles of Geology of the Granitic Pegmatites*. Nedra, Moscow, Russia (in Russ.).

GORDIYENKO, V.V. (1970): *Mineralogy, Geochemistry, and Genesis of the Spodumene-Bearing Pegmatites*. Nedra, Leningrad, Russia (in Russ.).

JAFFEY, A.H., FLYNN, K.F., GLENDENIN, L.E., BENTLEY, W.C. & ESSLING, A.M. (1971): Precision measurement of half-lives and specific activities of ^{235}U and ^{238}U. *Phys. Rev. C* **4**, 1889-1906.

JARDIM DE SÁ, E.F. (1984): Geologia da região do Seridó: reavaliaçõ de dados. *In* 11th Simp. Geol. Nordeste. *Soc. Bras. Geol.*, 278-296.

JARDIM DE SÁ, E.F. (1994): *A Faixa Seridó (Provincia Borborema NE do Brasil) e o seu significado geodinâmico na Cadeia Brasiliana/Pan-Africana, Brasília*. Ph.D. thesis, Univ. of Brasília, Brasília, Brazil.

JARDIM DE SÁ, E.F., LEGRAND, J.M. & MCREATH, I. (1981): "Estratigrafia" das rochas granitóides na região do Seridó (PB–RN) com base em critérios estruturais. *Rev. Brasil. Geocienc.* **11**, 50-57.

JARDIM DE SÁ, E.F., FUCK, R.A., MACEDO, M.H.F., PECAUT, J.J., KAWASHITA, K., SOUZA, Z.S. & BERTRAND, J.M. (1995): Pre-Brasiliano orogenic evolution in the Seridó Belt, NE Brazil: conflicting geochronological and structural data. *Rev. Brasil. Geosci.* **25**, 307-314.

JARDIM DE SÁ, E.F. & SALIM, J. (1980): Reavaliação dos conceitos estratigraficos na região do Seridó (RN/PB). *Mineração e Metalurgia* **80**, 16-28.

JOHNSTON, W.D., JR. (1945): Beryl–tantalite pegmatites of northeastern Brazil. *Geol. Soc. Am., Bull.* **56**, 1015-1070.

LEGRAND, J.M., LIEGEOIS, J.P. & DEUTSCH, S. (1991): Datação U–Pb e Rb–Sr das rochas pré-cambrianas da região de Caicó: re-avaliação da definição de um embrasamento arqueano. *In* 14th Simp. Geol. Nordeste. *Soc. Bras. Geol., Abstr.* **12**, 276-279.

LIMA, E.S. (1980): Projecto Scheelita do Seridó. Departamento Nacional de Produção Mineral, Serviço Geologico do Brasil, 35 vols.

LIMA, E.S. (1986): *Metamorphism and tectonic evolution in the Seridó region, northeastern Brazil*. Ph.D. thesis, University of California, Los Angeles, California.

LIMA, E.S. (1992): Metamorphic conditions in the Seridó region of northeastern Brazil during the Brasiliano cycle (Late Proterozoic). *J. S. Am. Earth Sci.* **5**, 265-273.

LONDON, D. (1990): Internal differentiation of rare-element pegmatites; a synthesis of recent research. *In* Ore-Bearing Granite Systems: Petrogenesis and Mineralizing Processes (H.J. Stein & J.L. Hannah, eds.). *Geol. Soc. Am., Spec. Pap.* **246**, 35-50.

LUDWIG K.R. (1999): Isoplot/Ex version 2.03. A geochronological tool kit for Microsoft Excel. *Berkeley Geochronological Center, Spec. Publ.* **1**, 1-43.

MORTEANI, G., PREINFALK, C. & HORN, A.H. (2000): Classification and mineralization potential of the pegmatites of the Eastern Brazilian Pegmatite Province. *Mineral. Deposita* **35**, 638-655.

PUTZER, H. (1976): Metallogenetische Provinzen in Südamerika. *Zentralblatt für Geologie und Palaeontologie. I. Allgemeine, Angewandte, Regionale und Historische Geologie* **3-4**, 360-365.

ROLFF, P.A.M.A. (1946): Minerais dos pegmatitos da Borborema. *DNPM/DFPM* **78**, 24-76.

ROMER, R.L. (2003): Alpha-recoil in U–Pb geochronology: effective sample size matters. *Contrib. Mineral. Petrol.* **145**, 481-491.

ROMER, R.L., FÖRSTER, H.-J. & BREITKREUZ, C. (2001): Intracontinental extensional magmatism with a subduction fingerprint: the late Carboniferous Halle Volcanic Complex (Germany). *Contrib. Mineral. Petrol.* **141**, 201-221.

ROMER, R.L. & SMEDS, S.-A. (1996): U–Pb columbite ages of pegmatites from Sveconorwegian terranes in southwestern Sweden. *Precamb. Res.* **76**, 15-30.

ROMER, R.L. & WRIGHT, J.E. (1992): U–Pb dating of columbites: a geochronologic tool to date magmatism and ore deposits. *Geochim. Cosmochim. Acta* **56**, 2137-2142.

SALIM, J. (1979): *Geologia e contrôle das mineralizações scheeltíferas da região da Serra de Feiticeiro e Bonfim, Lages-RN*. M.Sc. thesis, University of Brasília, Brasília, Brazil.

SCHOBBENHAUS, C. (1984): Distribution of mineral deposits through geologic time in Brazil. *Int. Geol. Congress, 27th (Moscow)*, 289.

SMITH, S.R., FOSTER, G.L., ROMER, R.L., TINDLE, A.G., KELLEY, S.P., NOBLE, S.R., HORSTWOOD, M. & BREAKS, F.W. (2004): U–Pb columbite–tantalite chronology of rare-element pegmatites using TIMS and laser ablation-multicollector ICP–MS. *Contrib. Mineral. Petrol.* **147**, 549-564.

SOUZA NETO, J.A. (1999): *Genesis of the Bonfim and Itajubatiba gold skarn deposits, northeastern Brazil: a study based on isotopes, trace elements and fluid inclusions*. Thèse de doctorat, Univ. Louvain-la-Neuve, Belgique.

STEIGER, R.H. & JÄGER, E. (1977): Subcommission on geochronology: convention on the use of decay constants in geo- and cosmochronology. *Earth Planet. Sci. Lett.* **36**, 359-362.

VAN SCHMUS, W.R, DANTAS, E., FETTERA, A., BRITO NEVES, B.B., HACKSPACHER, P.C. & BABINSKI, M. (1996): Neoproterozoic age for Seridó Group, NE Borborema Province, Brazil. *In* Cong. Bras. Geol. (Salvador-BA). *Soc. Bras. Geol.* **6**, 152-155.

ZARTMAN, R.E. & DOE, B.R. (1981): Plumbotectonics – the model. *Tectonophysics* **75**, 135-162.

Received June 2, 2005, revised manuscript accepted January 6, 2006.